doi:10.1016/j.jmb.2010.09.054 J. Mol. Biol. (2010) 404, 328–336

Contents lists available at www.sciencedirect.com

Journal of Molecular Biology

journal homepage: http://ees.elsevier.com.jmb

A pH-Dependent Dimer Lock in Spider Silk Protein

Michael Landreh[1]*, Glareh Askarieh[2,3], Kerstin Nordling[4], My Hedhammar[4], Anna Rising[4], Cristina Casals[5], Juan Astorga-Wells[1], Gunvor Alvelius[1], Stefan D. Knight[3], Jan Johansson[4], Hans Jörnvall[1] and Tomas Bergman[1]

[1]*Division of Chemistry I, Department of Medical Biochemistry and Biophysics, Karolinska Institutet, SE-171 77 Stockholm, Sweden*
[2]*Department of Chemistry, Oslo University, 1033 Blindern, 0315 Oslo, Norway*
[3]*Department of Molecular Biology, Swedish University of Agricultural Sciences, The Biomedical Center, SE-751 23 Uppsala, Sweden*
[4]*Department of Anatomy, Physiology, and Biochemistry, Swedish University of Agricultural Sciences, The Biomedical Center, SE-751 23 Uppsala, Sweden*
[5]*Department of Biochemistry and Molecular Biology I, and CIBER Enfermedades Respiratorias, Complutense University of Madrid, 28040 Madrid, Spain*

Received 17 May 2010; received in revised form 21 September 2010; accepted 23 September 2010
Available online 29 September 2010

Edited by F. Schmid

Keywords:
spidroins;
pH dependence;
electrospray ionization mass spectrometry;
protein–protein interactions;
hydrogen/deuterium exchange

Spider dragline silk, one of the strongest polymers in nature, is composed of proteins termed major ampullate spidroin (MaSp) 1 and MaSp2. The N-terminal (NT) domain of MaSp1 produced by the nursery web spider *Euprosthenops australis* acts as a pH-sensitive relay, mediating spidroin assembly at around pH 6.3. Using amide hydrogen/deuterium exchange combined with mass spectrometry (MS), we detected pH-dependent changes in deuterium incorporation into the core of the NT domain, indicating global structural stabilization at low pH. The stabilizing effects were diminished or abolished at high ionic strength, or when the surface-exposed residues Asp40 and Glu84 had been exchanged with the corresponding amides. Nondenaturing electrospray ionization MS revealed the presence of dimers in the gas phase at pH values below—but not above—6.4, indicating a tight electrostatic association that is dependent on Asp40 and Glu84 at low pH. Results from analytical ultracentrifugation support these findings. Together, the data suggest a mechanism whereby lowering the pH to <6.4 results in structural changes and alteration of charge-mediated interactions between subunits, thereby locking the spidroin NT dimer into a tight entity important for aggregation and silk formation.

Introduction

Spider silk is one of the toughest polymers found in nature and is adaptable to a broad range of biological functions. Dragline silk consists of spidroins produced by the major ampullate gland. The proteins can be stored in a highly concentrated soluble state ('dope') in the gland's sac. During spinning, the dope passes from the sac through a duct and is converted into an insoluble fiber.[1] Over

*Corresponding author. E-mail address: Michael.Fitzen@ki.se.

Abbreviations used: MaSp, major ampullate spidroin; NT, N-terminal; MS, mass spectrometry; ESI, electrospray ionization; wt, wild type; HDX, hydrogen/deuterium exchange; CID, collision-induced dissociation.

the length of the passage, the protein dope undergoes a pH drop from pH 6.9 in the sac to pH 6.3 in the distal region of the duct.[2] This pH drop, along with altered salt concentration, dehydration, and shear forces, is involved in the assembly of soluble spidroins into fibrils.[3]

Major ampullate spidroin (MaSp) contains ~3500 residues and can be divided into a highly conserved N-terminal (NT) domain of ~130 residues, a long repetitive middle section composed of poly-Ala-rich and Gly-rich segments, and a less conserved C-terminal domain containing ~110 residues.[4,5] The NT domain is associated with the pH dependency of fibril formation, the repetitive region affects the mechanical characteristics of spider silk, and the C-terminal domain governs assembly, preventing unordered aggregation.[6,7] Investigations carried out with recombinant forms of MaSp1 from the nursery web spider *Euprosthenops australis* have shown that assembly is independent of pH when the NT domain is removed, while inclusion of the NT domain restores pH dependency,[6,8,9] making it essential to study how this dependency is mediated.

In solution, the recombinant MaSp1 NT domain (residues 5–136)[8] assembles into large complexes with a hydrodynamic size of ~700 nm as pH is decreased below 6.4. Complex formation can be reversed by increasing the pH, while high levels of salt inhibit assembly. The crystal structure of the spidroin NT domain was recently determined and reveals a homodimeric conformation, where each subunit is composed of a five-helix bundle.[8] Notable is the uneven distribution of surface-exposed charged residues forming a positive pole and a negative pole in each subunit. The two subunits are arranged with their dipole axes in opposite directions.

To obtain a dynamic view of spidroin NT domain interactions in response to pH changes, we applied electrospray ionization (ESI) mass spectrometry (MS) to wild-type (wt) and mutant forms of the spidroin NT domain in the pH interval 6.0–7.0. ESI-MS was selected since noncovalent protein–protein interactions can be preserved and studied in the gas phase to reveal stoichiometries, apparent dissociation constants, and interaction modes for protein complexes.[10,11] Amide hydrogen/deuterium exchange (HDX), in combination with ESI-MS (HDX-MS),[12–14] gives information about conformational changes and structural flexibility by measurement of differential deuterium incorporation into protein backbone amides. Flexible or solvent-exposed segments allow rapid exchange, while less exposed or tightly folded segments exchange more slowly. The various degrees of deuterium incorporation into protein segments were determined using peptic digestion and LC-MS analysis[14–16] to identify pH-dependent changes in secondary structure elements and local conformation. Analytical ultracentrifugation was employed to correlate gas-phase data with solution data. The results show that a drop in pH causes global stabilization and charge-dependent locking of the dimer, providing insight into the mechanism behind spidroin assembly.

Results

Gas-phase interactions of the spidroin NT domain

Nondenaturing ESI-MS analysis of the wt spidroin NT domain in ammonium acetate at pH values ranging from 6.0 to 7.0 was carried out in steps of 0.2 pH unit (Fig. 1a). At pH 6.4–7.0, mainly monomeric protein was observed in the gas phase, while at pH 6.2 and 6.0, a large increase in gas-phase-stable dimers could be detected. Collision-induced dissociation (CID) experiments showed that these dimers require collision energies above 40 eV to partially dissociate, indicating strong interactions (Supplementary Fig. 1).

To investigate the influence of charged residues on the formation of dimers observed in the gas phase, we studied a set of spidroin NT domain mutants where the highly conserved and surface-exposed residues Asp40 and Glu84 had been exchanged with Asn (D40N) and Gln (E84Q), respectively. A double mutant (D40N/E84Q), as well as a mutant where Glu79 (not at the surface) had been changed to Gln (E79Q), was also studied. When the pH was changed from 7.0 to 6.0, only a limited amount of E84Q dimers was detected at low pH, while D40N and the double mutant D40N/E84Q were not able to form dimers that can be transferred to the gas phase at any pH (Fig. 1b). E79Q, on the other hand, revealed pH-dependent dimers at low pH in the ESI-MS spectra. For this mutant, dimerization was also observed at pH 6.8 and 7.0, but to a lower extent than at low pH (Fig. 1b).

Analytical ultracentrifugation and sedimentation equilibrium experiments

To correlate the gas-phase data with the solution data, we carried out ultracentrifugation experiments (Fig. 2). At pH 7.2, the wt spidroin NT domain revealed a sedimentation coefficient (s) of 1.7 ± 0.1 S; at pH 6.2, the s-value was 2.8 ± 0.1 S. Parallel sedimentation equilibrium experiments were performed to determine the mass of the main molecular species in solution. At pH 7.2, we found an average mass of 17,470 ± 998 Da, which is slightly greater than the calculated molecular mass of 14,011 Da for the monomeric wt spidroin NT domain. At pH 6.2, the average molecular mass of the wt spidroin NT domain was determined to be 25,450 ± 372 Da, which is most compatible with the size expected of a dimer. The ultracentrifugation data are thus in line with the

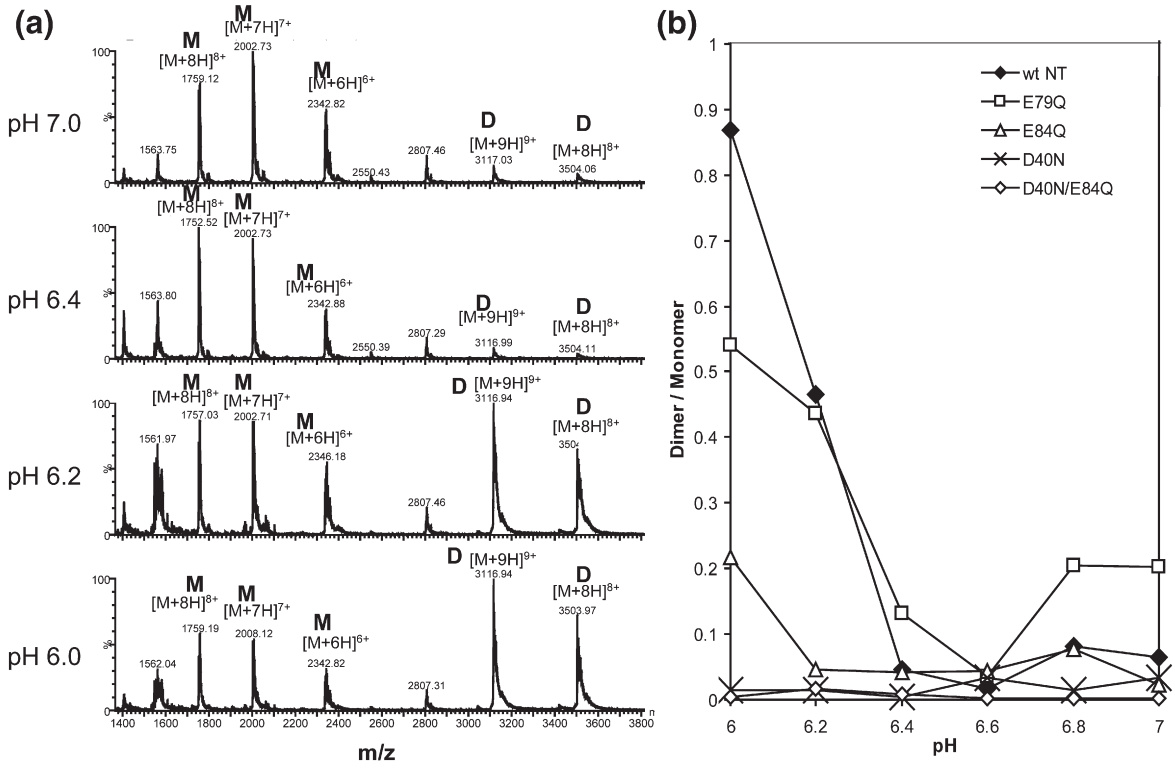

Fig. 1. ESI-MS spectra showing the pH-dependent dimer formation of wt and mutant spidroin NT domains. (a) ESI-MS spectra of the wt spidroin NT domain at pH values between 7.0 and 6.0. Peaks corresponding to monomers and dimers are denoted M and D, respectively. (b) Plot of the observed dimer/monomer gas-phase ratios of the wt spidroin NT domain and the E79Q, E84Q, D40N, and D40N/E84Q mutants. While D40N and D40N/E84Q do not show a pH-dependent increase in dimers at low pH, a small increase was observed for the E84Q mutant at pH 6.0. The E79Q mutant shows a pH-dependent increase in dimers at low pH; however, dimers could also be detected at pH 7.0 and 6.8.

observations made in the gas phase (i.e., the wt spidroin NT domain forms mainly dimers at acidic pH while being mainly monomeric at neutral pH).

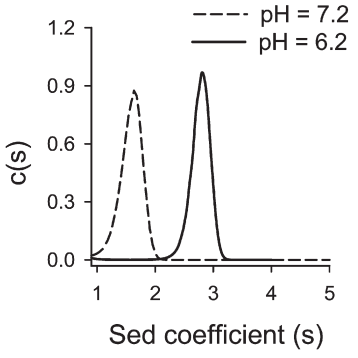

Fig. 2. Sedimentation velocity analysis of the wt spidroin NT domain at neutral and acidic pH values. The protein exhibits a peak with a sedimentation coefficient of 1.7 ± 0.1 S at neutral pH and a sedimentation coefficient of 2.8 ± 0.1 S at acidic pH, indicating molecular masses of 17,470 ± 998 and 25,450 ± 372 Da, respectively. The results shown are representative of one of three experiments.

Deuterium incorporation into wt spidroin NT domain

The spidroin NT domain was subjected to HDX-MS experiments at pH 7.0 and 6.0. Due to the relatively small size of the spidroin NT domain (14,011 Da), 93% of the protein sequence was covered in a limited number of peptic fragments with isolated MS signals. Since the backbone amide HDX rate is slowed by 1 order of magnitude when the pH is lowered from 7.0 to 6.0, the incubation times at pH 6.0 were extended by a factor of 10 for a direct comparison with deuterium incorporation at pH 7.0.[15,16]

Deuteration profiles for wt spidroin NT domain at pH 7.0 and 6.0 (Fig. 3, top and middle) both show that the deuteration level at a given time point varies along the polypeptide chain, and that regions with low levels of deuterium labeling coincide with the positions of the five α-helices determined by X-ray crystallography.[8] Since α-helices are known to incorporate deuterium more slowly than unfolded segments, we conclude that these regions of the backbone are in α-helical conformation and, thus,

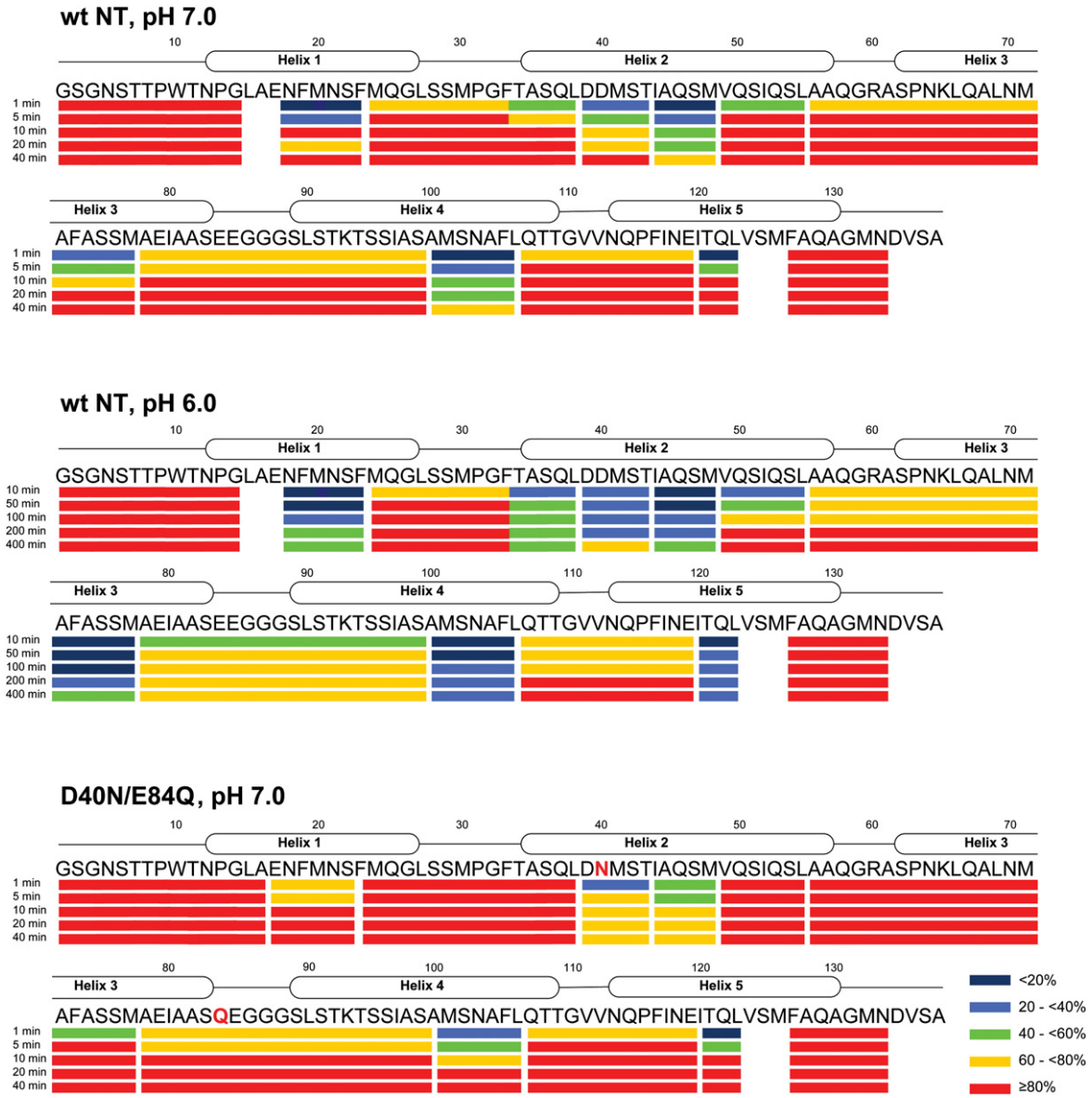

Fig. 3. Deuterium exchange profiles for wt and mutant spidroin NT domains. Profiles are shown for wt spidroin NT domain at pH 7.0 (top) and pH 6.0 (middle), and for D40N/E84Q at pH 7.0 (bottom; mutated positions are indicated in red). Incorporation of deuterium after various incubation times is indicated by color-coded underlining of the amino acid sequence. Each line corresponds to an observed peptic fragment. The corresponding deuteration levels (in percent) are given on the bottom right. The positions of the five α-helices are indicated. Residue numbering follows Askarieh *et al.*[8]

that the positions of the five α-helices are not significantly altered by the pH shift. On the other hand, the deuteration levels differ significantly between pH 7.0 and pH 6.0, in particular for regions that exchange slowly. At pH 6.0, deuterium incorporation into all helical segments is lower than at pH 7.0. This observation indicates decreased unfolding and tighter packing of these regions at low pH.

To visualize pH-dependent local perturbations, we calculated the average differences in deuterium incorporation between pH 7.0 and pH 6.0 using data for all time points[17,18] (Fig. 4). Positive perturbations, reflecting increased solvent exposure and structural flexibility in response to lowered pH, were not observed. In contrast, negative perturbations, reflecting structural stabilization and shielding from the solvent, could be observed for the middle regions of all helices, corresponding to the hydrophobic core of the spidroin NT domain (Fig. 5). The strongest negative perturbation was observed for the middle segment of helix 3, a region shown by crystallography to be buried at the interface between the dimer subunits.[8]

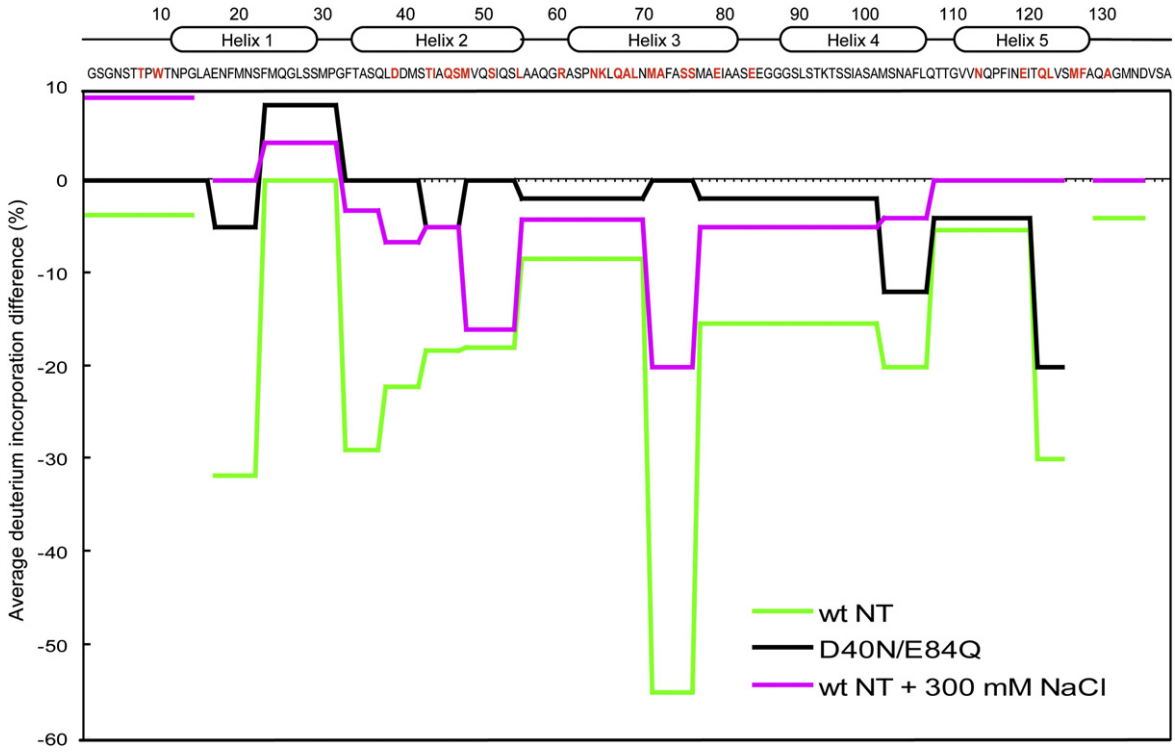

Fig. 4. Changes in average deuterium incorporation in response to lowered pH. Perturbations (from 7.0 to 6.0) were calculated for the wt spidroin NT domain, the D40N/E84Q mutant, and the wt spidroin NT domain in the presence of 300 mM NaCl. Negative perturbations indicate less deuterium exchange at lower pH. Residues located at the dimer interface are indicated in red. Residue numbering follows Askarieh *et al.*[8]

Deuterium exchange in the D40N/E84Q mutant

The deuterium incorporation profiles of the D40N/E84Q double mutant reveal regions with deuteration levels lower than those for neighboring segments (Fig. 3, bottom). As for the wt spidroin NT domain, these regions coincide with the positions of α-helices, in agreement with the observation that the structure of the D40N/E84Q double mutant is largely identical with that of the wt NT domain.[8] However, at pH 7.0, segments covering helices 1, 2, 3, and 4 were deuterated more rapidly in the NT domain double mutant than in the wt NT domain (Fig. 3; Supplementary Fig. 2), indicating that the mutant exhibits a higher unfolding rate in these regions at pH 7.0. Moreover, only minor differences were observed between the deuterium incorporation level at pH 7.0 and the deuterium incorporation level at pH 6.0 for the D40N/E84Q mutant (Fig. 4).

Effect of ionic strength on pH-dependent structural change

HDX-MS time-course experiments were performed with wt spidroin NT domain at pH 7.0 and 6.0 in the presence of 300 mM NaCl, and the resulting perturbations were determined (Fig. 4; Supplementary Fig. 2). Comparison of deuterium incorporation at pH 7.0 and 6.0 at high and low ionic strengths shows that high-salt conditions decrease the deuteration of helical segments at pH 7.0, while the deuteration levels at pH 6.0 are similar independent of salt concentration (Supplementary Fig. 2). Consequently, the perturbations going from pH 7.0 to pH 6.0 are less pronounced in the presence of 300 mM NaCl, indicating that the pH-dependent difference in structural flexibility is reduced at high ionic strength (Fig. 4).

Discussion

The NT domain of *E. australis* MaSp1 is involved in the pH-dependent regulation of spider silk assembly. The conserved overall structure of this domain shows a positive pole and a negative pole on the surface, suggesting that charge interactions play a role in the formation of spider silk in the extrusion duct of the ampullate gland.[8] Using MS, we have studied the effect of pH on the structural flexibility of the spidroin NT domain and investigated the role of conserved charged residues.

ESI-MS experiments showed that at pH values below—but not above—6.4, the spidroin NT

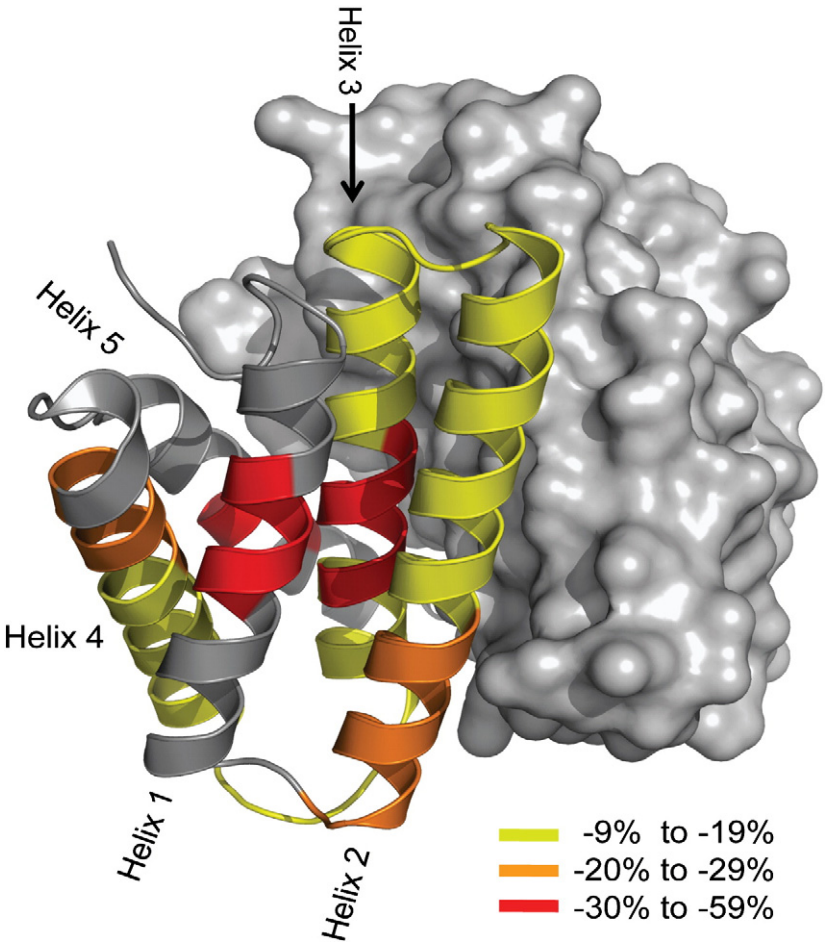

Fig. 5. Structural representation of the deuterium exchange profile for the wt spidroin NT domain. The negative perturbations observed in the wt protein (Fig. 4) are indicated in the crystal structure of the wt spidroin NT domain dimer (Protein Data Bank ID 3LR2[8]) according to the color code given. To visualize the domain organization of the spidroin NT domain dimer, we show one subunit as space-fill model, and we label the secondary structure elements as helices 1–5. Decreased deuteration levels can be observed in the core of the helix bundle composed of the middle regions of all five helices.

domain forms dimers that can be transferred to the gas phase (Fig. 1a). Hydrophobic interactions are known to be weakened in the gas phase, while electrostatic interactions are reinforced.[19] The high relative stability of the dimers observed below pH 6.4 and their dependency on the charged residues Asp40 and Glu84 therefore suggest that their association at low pH is dominated by electrostatic interactions.

To make a correlation with solution conditions at neutral pH *versus* solution conditions at acidic pH, we subjected the wt spidroin NT domain to analytical ultracentrifugation. It was found that the protein is primarily monomeric at pH 7.2, while it forms mainly dimers at pH 6.2 (Fig. 2). The data are thus in line with the results from gas-phase experiments. However, it should be noted that, in size-exclusion chromatography, the wt spidroin NT domain migrates primarily as a dimer, both at neutral pH and at acidic pH.[6]

It is interesting to note that the E79Q mutation has an effect different from the effects of the E84Q and D40N mutations. The D40N and E84Q mutants are not able to form dimers that, to a significant degree, are transferrable to the gas phase, while the E79Q mutant forms dimers that can be observed in the gas phase both at high pH and at low pH, with a minimum at pH 6.6 (Fig. 1b). Glu79 is a conserved residue, but it is not located at the surface of the protein.

Large assemblies of wt or mutant spidroin NT domains were not observed in the ESI-MS spectra. Such protein complexes are reported to have a hydrodynamic size of ~700 nm,[8] and it is unlikely that such assemblies survive the ESI process or are sufficiently ionized to be detected.

We carried out HDX-MS experiments to map differences in the deuteration levels of protein backbone amides in response to lowered pH. The distribution of slowly deuterated regions coincides with the distribution of α-helices in the crystal structure and suggests that the crystal structure of the spidroin NT subunit resembles that in solution.

The deuteration level of individual peptic peptides is represented for each peptide as percent maximum deuteration.[14,15,18,20] It is important to note that the resolution in the deuterium exchange profile is limited by the specificity and efficiency of the peptic digestion, and it is difficult to judge the distribution of deuterons in longer proteolytic

fragments. However, since comparisons are made for a particular peptic fragment at different time points and under different conditions, percent values are reasonable for judging the alteration of deuteration levels in segments of the protein backbone.

We observed that deuteration levels of segments from the hydrophobic core of the wt spidroin NT domain are decreased at low pH (Fig. 5). This indicates decreased unfolding rates in these regions and leads to the conclusion that the dimers transferred to the gas phase at low pH are tightly packed with reduced solvent accessibility. Mutation of the highly conserved residues Asp40 and Glu84 to the corresponding amides apparently reduces the structural stabilization at low pH. The observation that helix 3 displays the strongest negative perturbation of the entire spidroin NT domain (Fig. 4) can be explained by the fact that it is fully buried at the interface between the subunits and flanked by charged residues that are implicated in dimer locking.

Charge-dependent conformational changes are frequently altered by high ionic strength. We observed that, in the presence of 300 mM NaCl, the deuterium incorporation levels at pH 7.0 are reduced, while they are largely unchanged at pH 6.0, resulting in less pronounced pH-dependent structural perturbations (Fig. 4). This indicates that high-salt concentration leads to a more pH-independent conformation. This could be due to the masking of charge interactions in the spidroin NT domain that are required for the observed pH-dependent structural changes.

The dimer interface observed in the crystal structure of the spidroin NT domain harbors significantly more polar residues (43%) than the average homodimer interface (30%).[20] Hence, nonpolar interactions are expected to be relatively less important for the stabilization of the spidroin NT domain dimer. In the dimer structure, residues Asp40 and Glu84 from the same subunit form an intrasubunit "handshake" interaction.[8] The two residues are not positioned in a manner that allows dimer-stabilizing intersubunit interactions, suggesting that they are instead required for conformational changes needed for dimer stabilization. Examination of the spidroin NT domain dimer structure shows that many of the side chains at the interface have multiple conformations. A comparison of crystal structures for the wt spidroin NT domain dimer in two different crystal forms and for the spidroin NT domain mutants shows that the dimer subunits are able to rotate around a fairly flat interface.[8] Both of these observations suggest that the dimer interface is not entirely rigid. It is tempting to speculate about a scenario where multiple conformations are allowed at higher pH values, while a single more compact and assembly-competent conformation is stabilized by interactions involving Asp40 and Glu84 at pH values below 6.4.

In conclusion, we have presented evidence that the NT domain of MaSp1 from *E. australis* undergoes a pH-dependent electrostatic locking event leading to a globally stabilized dimer. The pH interval where this occurs coincides with the measured pH drop in the spinning duct of the spider, which strongly suggests that the assembly of spidroins involves the locking event of the spidroin dimer NT domain reported here.

Materials and Methods

Deuterium exchange

Wt and mutant NT domains from *E. australis* MaSp1 were expressed and purified as described previously.[6,8] Stock phosphate buffers at 20 mM were adjusted to pH 5.8 and 6.9. A mixture of 9 vol of stock phosphate buffer and 1 vol of protein stock solution (10 mg/ml spidroin NT domain in 20 mM Tris–HCl, pH 8.0) results in a final pH of 6.0 and 7.0, respectively. Deuterated buffers were prepared by four rounds of freeze-drying of the stock phosphate buffers and reconstitution in 99.9% D_2O (Cambridge Isotopes, Andover, MA). To start the incubation at 22 °C, we diluted the spidroin NT domain stock solution 10 times in deuterated stock phosphate buffer, resulting in a final deuterium content of about 90% and a protein concentration of 1 mg/ml. Time aliquots (4 μl) for ESI-MS analysis were collected from 1 min onwards. Deuterium exchange was quenched by the transfer of aliquots to prechilled Eppendorf tubes containing 16 μl of 0.1% trifluoroacetic acid (Merck, Darmstadt, Germany), vortexing for 2 s, and freezing in liquid nitrogen. Samples were kept in liquid nitrogen until analyzed.

Mass spectrometry

To investigate gas-phase protein–protein interactions, we diluted the spidroin NT domain stock solution 100-fold in 10 mM ammonium acetate buffers adjusted to pH 6.0, 6.2, 6.4, 6.6, 6.8, or 7.0 to yield solutions with a final protein concentration of 0.1 mg/ml. Samples were introduced into the mass spectrometer using metal-plated borosilicate glass capillary needles (Proxeon, Odense, Denmark).

For HDX-MS, aliquots of deuterated wt spidroin NT domain were quickly thawed and injected into an HPLC system using a prechilled Hamilton syringe. The entire system was submerged in an ice bath during analysis.[21] Protein samples were injected into a 5-μl sample loop and digested online in a Porozyme Immobilized Pepsin Cartridge (Applied Biosystems, Foster City, CA) operated at 17 μl/min in 0.05% trifluoroacetic acid. Peptic peptides were desalted using a Waters Symmetry C_{18} trap column and eluted in a single step with 70% acetonitrile containing 0.1% formic acid at a flow rate of 17 μl/min. Samples were delivered to the mass spectrometer through a tapered tip emitter with a 50-μm opening (New Objective, Milford, MA) coupled to the HPLC via a T-connector.

Spectra were acquired in positive-ion mode with a Waters Ultima API mass spectrometer (Waters, Milford, MA) equipped with a Z-spray source. The source temperature was 80 °C, the capillary voltage was 1.7 kV, and the cone and radiofrequency lens 1 potentials were 100 and 38 V, respectively. The mass spectrometer was operated in single-reflector mode to achieve a resolution of 10,000 (full width at half maximum). The mass scale was calibrated using myoglobin for gas-phase interaction experiments and using [Glu1]fibrinopeptide B for HDX-MS. Scans were acquired for 5 min at a rate of one scan per 2 s between 500 m/z and 4000 m/z for gas-phase interaction studies, and between 200 m/z and 2000 m/z for HDX-MS. Argon at 5.2×10^{-5} mbar was used in CID experiments. Mass spectra were analyzed using Waters MassLynx software. For determination of monomer/dimer ratios, ESI-MS spectra were smoothed (5 G) and centered, and ratios were calculated from the sum of the signal intensities of the $[M+6H]^{6+}$, $[M+7H]^{7+}$, and $[M+8H]^{8+}$ charge states of the monomer, and the $[M+8H]^{8+}$ and $[M+9H]^{9+}$ charge states of the dimer.[11]

To correct for back exchange, we prepared the fully deuterated protein by freeze-drying of a sample of spidroin NT domain followed by resuspension in 99.9% D_2O and 4 h of incubation at 50 °C. This procedure was repeated twice before the sample was subjected to online digestion and ESI-MS. Backexchange corrections and deuteration level calculations were performed as described previously.[14] Peptic peptides were identified based on a map of pepsin-digested undeuterated material using automated LC-MS/MS analysis with a Waters NanoAcquity system (Waters). Peptide sequences were identified by individual analysis of CID spectra using the Waters MassLynx and ProteinLynx software packages.

Analytical ultracentrifugation

Sedimentation velocity experiments were performed at 48,000 rpm and 22 °C in a Beckman XL-A ultracentrifuge (Beckman Coulter, Inc.) with a UV–Vis detector, using an An-50Ti rotor and double-sector 12-mm centerpieces of Epon charcoal, as previously reported.[22] Sedimentation profiles were registered every 5 min at 235, 260, or 280 nm. Experiments were carried out in duplicate at two protein concentrations (150 and 450 μg/ml) in 10 mM phosphate buffer at different pH values. Typically, samples were centrifuged at 3000 rpm for 2.5 min prior to ultracentrifugation experiments to remove polymerized protein. The sedimentation coefficient distributions were calculated by least-squares boundary modeling of sedimentation velocity data using the $c(s)$ method,[23] as implemented in the SEDFIT program from which the corresponding s-values were determined.

To determine the mass of the main protein species, we performed parallel sedimentation equilibrium experiments in 10 mM potassium phosphate, at different pH values, using the following protein concentrations: 75, 100, 150, 225, and 450 μg/ml. Ultracentrifugation was performed at 18,000, 25,000, and 45,000 rpm. The absorbance scans were recorded when sedimentation equilibrium had been reached. The buoyant molecular masses of the wt spidroin NT domain were determined by fitting a sedimentation equilibrium model of a single sedimenting solute to individual data using the program EQASSOC[24] or HeteroAnalysis.[25] These values were then converted into the corresponding average molecular masses by using 0.7192 ml/g as the partial specific volume of the wt spidroin NT domain, calculated from amino acid composition with the program SEDNTERP.[26]

Supplementary data associated with this article can be found, in the online version, at doi:10.1016/j.jmb.2010.09.054

Acknowledgements

This work was supported by Swedish Research Council grants 13X-10371 and 03X-3532, the Neuroscience Network at Karolinska Institutet, and a Karolinska Institutet PhD student grant to M.L. J.A.-W. thanks Biomotif AB (Solna, Sweden) for support.

References

1. Work, R. W. (1977). Mechanisms of major ampullate silk fiber formation by orb-web-spinning spiders. *Trans. Am. Microsc. Soc.* **96**, 170–189.
2. Dicko, C., Vollrath, F. & Kenney, J. M. (2004). Spider silk protein refolding is controlled by changing pH. *Biomacromolecules*, **5**, 704–710.
3. Rising, A., Widhe, M., Johansson, J. & Hedhammar, M. (2010). Spider silk proteins: recent advances in recombinant production, structure–function relationships and biomedical applications. *Cell. Mol. Life Sci.* doi:10.1007/s00018-010-0462-z.
4. Rising, A., Hjalm, G., Engström, W. & Johansson, J. (2006). N-terminal nonrepetitive domain common to dragline, flagelliform, and cylindriform spider silk proteins. *Biomacromolecules*, **7**, 3120–3124.
5. Ayoub, N. A., Garb, J. E., Tinghitella, R. M., Collin, M. A. & Hayashi, C. Y. (2007). Blueprint for a high-performance biomaterial: full-length spider dragline silk genes. *PLoS One*, **2**, e514.
6. Hedhammar, M., Rising, A., Grip, S., Martinez, A. S., Nordling, K., Casals, C. *et al.* (2008). Structural properties of recombinant nonrepetitive and repetitive parts of major ampullate spidroin 1 from *Euprosthenops australis*: implications for fiber formation. *Biochemistry*, **47**, 3407–3417.
7. Sponner, A., Vater, W., Rommerskirch, W., Vollrath, F., Unger, E., Grosse, F. & Weisshart, K. (2005). The conserved C-termini contribute to the properties of spider silk fibroins. *Biochem. Biophys. Res. Commun.* **338**, 897–902.
8. Askarieh, G., Hedhammar, M., Nordling, K., Saenz, A., Casals, C., Rising, A. *et al.* (2010). Self-assembly of spider silk proteins is controlled by a pH-sensitive relay. *Nature*, **465**, 236–238.
9. Hagn, F., Eisoldt, L., Hardy, J. G., Vendrely, C., Coles, M., Scheibel, T. & Kessler, H. (2010). A conserved spider silk domain acts as a molecular switch that controls fibre assembly. *Nature*, **465**, 239–242.

10. Benesch, J. L. & Robinson, C. V. (2006). Mass spectrometry of macromolecular assemblies: preservation and dissociation. *Curr. Opin. Struct. Biol.* **16**, 245–251.
11. Fitzen, M., Alvelius, G., Nordling, K., Jörnvall, H., Bergman, T. & Johansson, J. (2009). Peptide-binding specificity of the prosurfactant protein C Brichos domain analyzed by electrospray ionization mass spectrometry. *Rapid Commun. Mass Spectrom.* **23**, 3591–3598.
12. Wales, T. E. & Engen, J. R. (2006). Hydrogen exchange mass spectrometry for the analysis of protein dynamics. *Mass Spectrom. Rev.* **25**, 158–170.
13. Englander, S. W., Mayne, L., Bai, Y. & Sosnick, T. R. (1997). Hydrogen exchange: the modern legacy of Linderström–Lang. *Protein Sci.* **6**, 1101–1109.
14. Zhang, Z. & Smith, D. L. (1993). Determination of amide hydrogen exchange by mass spectrometry: a new tool for protein structure elucidation. *Protein Sci.* **2**, 522–531.
15. Wang, L., Lane, L. C. & Smith, D. L. (2001). Detecting structural changes in viral capsids by hydrogen exchange and mass spectrometry. *Protein Sci.* **10**, 1234–1243.
16. Man, P., Montagner, C., Vernier, G., Dublet, B., Chenal, A., Forest, E. & Forge, V. (2007). Defining the interacting regions between apomyoglobin and lipid membrane by hydrogen/deuterium exchange coupled to mass spectrometry. *J. Mol. Biol.* **368**, 464–472.
17. Maegawa, G. H., Tropak, M. B., Buttner, J. D., Rigat, B. A., Fuller, M., Pandit, D. *et al.* (2009). Identification and characterization of ambroxol as an enzyme enhancement agent for Gaucher disease. *J. Biol. Chem.* **284**, 23502–23516.
18. Kornhaber, G. J., Tropak, M. B., Maegawa, G. H., Tuske, S. J., Coales, S. J., Mahuran, D. J. & Hamuro, Y. (2008). Isofagomine induced stabilization of glucocerebrosidase. *ChemBioChem*, **9**, 2643–2649.
19. Daniel, J. M., Friess, S. D., Rajagopalan, S., Wendt, S. & Zenobi, R. (2002). Quantitative determination of noncovalent binding interactions using soft ionization mass spectrometry. *Int. J. Mass Spectrom.* **216**, 1–27.
20. Reynolds, C., Damerell, D. & Jones, S. (2009). ProtorP: a protein–protein interaction analysis server. *Bioinformatics*, **25**, 413–414.
21. Jørgensen, T. J., Gardsvoll, H., Dano, K., Roepstorff, P. & Ploug, M. (2004). Dynamics of urokinase receptor interaction with peptide antagonists studied by amide hydrogen exchange and mass spectrometry. *Biochemistry*, **43**, 15044–15057.
22. Casals, C., Johansson, H., Saenz, A., Gustafsson, M., Alfonso, C., Nordling, K. & Johansson, J. (2008). C-terminal, endoplasmic reticulum-lumenal domain of prosurfactant protein C—structural features and membrane interactions. *FEBS J.* **275**, 536–547.
23. Schuck, P., Perugini, M. A., Gonzales, N. R., Howlett, G. J. & Schubert, D. (2002). Size-distribution analysis of proteins by analytical ultracentrifugation: strategies and application to model systems. *Biophys. J.* **82**, 1096–1111.
24. Minton, A. P. (1997). Alternative strategies for the characterization of associations in multicomponent solutions via measurement of sedimentation equilibrium. *Prog. Colloid Polym. Sci.* **107**, 11–19.
25. Cole, J. L. (2004). Analysis of heterogeneous interactions. *Methods Enzymol.* **384**, 212–232.
26. Laue, T. M., Shah, B. D., Ridgeway, T. M. & Pelletier, S. L. (1992). Interpretation of analytical sedimentation data for proteins. In (Harding, S. E., Rowe, A. J. & Horton, J., eds), Royal Society of Chemistry, Cambridge, UK.